OXFORD

Human Molecular Genetics, 2017, Vol. 26, No. 3 624–636

doi: 10.1093/hmg/ddw421
Advance Access Publication Date: 28 December 2016
Original Article

ORIGINAL ARTICLE

The roles of USH1 proteins and PDZ domain-containing USH proteins in USH2 complex integrity in cochlear hair cells

Junhuang Zou[1], Qian Chen[1], Ali Almishaal[2], Pranav Dinesh Mathur[1,3], Tihua Zheng[1,†], Cong Tian[4,‡], Qing Y. Zheng[4] and Jun Yang[1,3,5,*]

[1]Department of Ophthalmology and Visual Sciences, Moran Eye Center, University of Utah, Salt Lake City, UT 84132, USA, [2]Department of Communication Sciences and Disorders, University of Utah, 390 South 1530 East, Salt Lake City, UT 84112, USA, [3]Department of Neurobiology and Anatomy, University of Utah, 20 North 1900 East, Salt Lake City, UT 84132, USA, [4]Department of Otolaryngology, Case Western Reserve University, Cleveland, OH 44106, USA and [5]Division of Otolaryngology, Department of Surgery, University of Utah, 50 North Medical Drive, Salt Lake City, UT 84132, USA

*To whom correspondence should be addressed at: Jun Yang, Ph.D., John A Moran Eye Center, University of Utah, 65 Mario Capecchi Drive, Bldg 523, Salt Lake City, Utah 84132. Tel: 801-213-2591; email: jun.yang@hsc.utah.edu

Abstract

Usher syndrome (USH) is the most common cause of inherited deaf-blindness, manifested as USH1, USH2 and USH3 clinical types. The protein products of USH2 causative and modifier genes, *USH2A*, *ADGRV1*, *WHRN* and *PDZD7*, interact to assemble a multiprotein complex at the ankle link region of the mechanosensitive stereociliary bundle in hair cells. Defects in this complex cause stereociliary bundle disorganization and hearing loss. The four USH2 proteins also interact *in vitro* with USH1 proteins including myosin VIIa, USH1G (SANS), CIB2 and harmonin. However, it is unclear whether the interactions between USH1 and USH2 proteins occur *in vivo* and whether USH1 proteins play a role in USH2 complex assembly in hair cells. In this study, we identified a novel interaction between myosin VIIa and PDZD7 by FLAG pull-down assay. We further investigated the role of the above-mentioned four USH1 proteins in the cochlear USH2 complex assembly using USH1 mutant mice. We showed that only myosin VIIa is indispensable for USH2 complex assembly at ankle links, indicating the potential transport and/or anchoring role of myosin VIIa for USH2 proteins in hair cells. However, myosin VIIa is not required for USH2 complex assembly in photoreceptors. We further showed that, while PDZ protein harmonin is not involved, its paralogous USH2 proteins, PDZD7 and whirlin, function synergistically in USH2 complex assembly in cochlear hair cells. In summary, our studies provide novel insight into the functional relationship between USH1 and USH2 proteins in the cochlea and the retina as well as the disease mechanisms underlying USH1 and USH2.

[†]Present address: Transformative Otology and Neuroscience Center, Binzhou medical University, Yantai 264003, Shandong, Peoples Republic of China.
[†]Present address: Graduate School of Biomedical Science and Engineering, University of Maine, Bar Harbor, ME 04609, USA.
Received: November 17, 2016. **Revised:** November 17, 2016. **Accepted:** December 7, 2016

Introduction

Usher syndrome (USH) is the leading cause of inherited deaf-blindness, with a prevalence of 1 in 6000 people worldwide (1–4). Among the three clinical types of USH, type 1 (USH1) is the most severe form, characterized by congenital profound deafness, vestibular areflexia and onset of retinal degeneration (*i.e.* retinitis pigmentosa) before 10 years of age. Type 2 (USH2) is the most common form and manifests as congenital moderate to severe hearing impairment, little balance problem and onset of retinitis pigmentosa by the teenage years. The molecular basis underlying these USH clinical types is not completely understood, and there is no cure available (5).

In the inner ear, the stereociliary bundle on the apex of cochlear hair cells is the critical structure for mechanotransduction (6–8). This structure has three graded rows of actin-based stereocilia and one transient microtubule-based kinocilium. ADGRV1, usherin and whirlin are the protein products of the USH2 causative genes, *ADGRV1*, *USH2A* and *WHRN*, respectively, and PDZD7 is the protein product of the USH2 modifier gene, *PDZD7* (9–12). The four USH2 proteins interact with one another and constitute a multiprotein complex, the USH2 complex (also known as ankle link complex), at the cytoplasmic region of ankle links (13–16), which are a mesh of thin fibers connecting stereocilia at their bases and exist only during development (17). Defects in the USH2 protein complex cause disorganization of the stereociliary bundle, loss of individual stereocilia or entire stereociliary bundle and eventually hearing loss (13,18–21). The proteins encoded by USH1 genes also interact with one another and form various multiprotein complexes and interstereociliary links in the stereociliary bundle. For example, harmonin, USH1G and myosin VIIa form a complex at the upper tip link density (UTLD) and are involved in adaption of mechanotransduction in mature hair cells (22–29).

Interestingly, biochemical assays have demonstrated that USH2 proteins interact directly *in vitro* with USH1 proteins including myosin VIIa, USH1G, harmonin and CIB2 (13,30–32). However, no studies have been conducted to systematically examine the role of the USH1 proteins in USH2 complex assembly during hair cell stereociliary bundle development. Furthermore, harmonin, which has three PDZ domains, is paralogous to USH2 scaffold proteins, PDZD7 and whirlin (12,14,33). Whether these three paralogous PDZ domain-containing proteins function together in cochlear hair cells have not yet been explored. In this study, we investigated the effect of loss of USH1 proteins on the assembly of the USH2 complex in cochlear hair cells during development. We focused on the USH1 proteins known to interact with USH2 proteins. We also carefully compared the USH2 complex defects in *Pdzd7* and *Whrn* single- and double-mutant cochlear hair cells. Our findings provide novel insight into the functional relationship between USH1 and USH2 proteins and the molecular pathogenesis underlying USH1 and USH2. This knowledge might help future development of mechanism-based therapies for USH1 and USH2.

Results

Myosin VIIa interacts with the PDZ domains of PDZD7

Myosin VIIa, encoded by the *USH1B* gene, was previously shown to interact directly with ADGRV1, usherin and whirlin (13,34). In this study, we investigated whether myosin VIIa also interacted with PDZD7. We double-transfected HEK293 cells with a FLAG-tagged myosin VIIa fragment without the ATPase motor domain (the myosin VIIa tail) and GFP-tagged PDZD7 fragments (Fig. 1A). FLAG pull-down experiments (Fig. 1B) demonstrated that myosin VIIa tail was able to pull down full-length PDZD7 protein as well as the PDZD7 PDZ1 and PDZ3 fragments. Myosin VIIa tail was unable to pull down the PDZD7 PDZ2 fragment and the negative control GFP

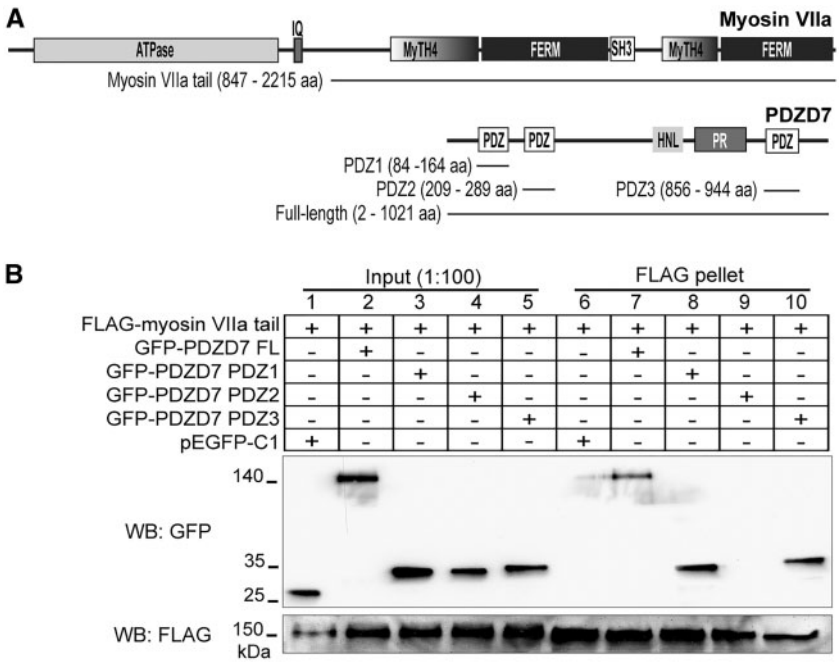

Figure 1. Myosin VIIa interacts with PDZD7. (**A**) Domain organization of myosin VIIa and PDZD7. Lines below each diagram indicate the myosin VIIa and PDZD7 fragments used in this study. (**B**) FLAG-myosin VIIa tail pulled down GFP-PDZD7 full-length (FL, lane 7), PDZ1 (lane 8) and PDZ3 (lane 10) proteins, but not GFP-PDZD7 PDZ2 (lane 9) or GFP (pEGFP-C1, lane 6) protein. The lower anti-FLAG blot demonstrates the success of the FLAG pull-down assay. Lanes 1-5 are input samples showing the presence of the transfected proteins in cell lysates. + and -, presence and absence of proteins in the transfected cells, respectively.

protein. Therefore, myosin VIIa is able to interact with PDZD7 through its PDZ1 and PDZ3 domains but not its PDZ2 domain.

Myosin VIIa determines the distribution of the four USH2 proteins at the ankle link region in cochlear hair cells

Because myosin VIIa is able to interact with all four USH2 proteins *in vitro*, we studied the role of myosin VIIa in the localization of the USH2 complex during cochlear hair cell development using *Myo7a*$^{sh1\text{-}7J}$*/J* (referred to hereafter as *Myo7a*$^{7J/7J}$) mice. We identified the *Myo7a*$^{7J/7J}$ mutation by reverse transcription-polymerase chain reaction (RT-PCR). DNA sequencing analysis of the RT-PCR product generated from *Myo7a*$^{7J/7J}$ retinas by primers 7F and 13R (Supplementary Material, Table S1) identified a 778-bp deletion between 4349 and 5126 bp (c.4349_5126del, pAla1363AlafsTer27) in myosin VIIa transcript 2 (NM_008663) (Supplementary Material, Fig. S1), the major myosin VIIa transcript in the retina and the inner ear. This mutation is also equivalent to an 892-bp deletion between 4349 and 5240 bp (c.4349_5240del, pAla1363AlafsTer27) in myosin VIIa transcript 1 (NM_001256081), which was also expressed in the inner ear. The *Myo7a*$^{7J/7J}$ mutation is expected to cause a reading frame shift and premature truncation of the protein immediately after the myosin VIIa motor. RT-PCR using primers at other regions of the gene produced products of similar size from *Myo7a*$^{+/7J}$ and *Myo7a*$^{7J/7J}$ retinal cDNAs. Immunostaining using our myosin VIIa antibody, which detects the N-terminal region of myosin VIIa (1 -997 aa), showed that *Myo7a*$^{7J/7J}$ cochlear hair cells lack immunoreactivity at the stereociliary bundle, while the immunoreactivity was seen in the stereociliary bundle of wild-type mice (Supplementary Material, Fig. S1C), indicating that a significantly low level or none of truncated myosin VIIa protein is expressed in *Myo7a*$^{7J/7J}$ cochlear hair cells.

The *Myo7a*$^{7J/7J}$ cochlear hair cells showed elongated, splayed and disorganized stereocilia, visualized by actin-staining with phalloidin (Fig. 2), similar to those previously reported in other *Myo7a* mutant strains (35,36). To avoid the confounding effect of secondary defects due to the severe morphological defects in *Myo7a*$^{7J/7J}$ cochlear stereociliary bundles, we performed our experiments at postnatal day 4 (P4), 2 days after the formation of the USH2 complex, when the USH2 protein signals just become robust (13,15–18,34,37). Compared with wild-type cochleas (Fig. 2A), the vast majority of ADGRV1 immunoreactivity was mislocalized as large punctate signals on the apical surface of hair cells [91.1% of inner hair cells (IHCs) and 83.6% of outer hair cells (OHCs)] in the entire *Myo7a*$^{7J/7J}$ cochleas, while residual ADGRV1 immunoreactivity also remained at some ankle links (73.7% of IHCs and 62.7% of OHCs) and/or was mislocalized at the stereociliary tips (17.5% of IHCs and 9.6% of OHCs) (Fig. 2B and Supplementary Material, Table S2). The usherin fluorescent signal largely disappeared in *Myo7a*$^{7J/7J}$ IHC (100%) and OHC (100%) stereociliary bundles (Fig. 2C and Supplementary Material, Table S2). These ADGRV1 and usherin signal patterns were consistent with a previous report in the IHCs of a different *Myo7a* mutant mouse line *Myo7a*^{4626SB} at P6 (13). The distributions of whirlin and PDZD7 were also affected in the absence of myosin VIIa. The whirlin signal was significantly decreased (32.4% of IHCs and 53.8% of OHCs) or absent (61.8% of IHCs and 30.8% of OHCs) at the ankle link region, *i.e.* the base of the stereocilia, but remained at the stereociliary tip in both IHCs and OHCs (Fig. 2D and Supplementary Material, Table S2). The PDZD7 immunoreactivity was barely detectable at the stereociliary bundles of *Myo7a*$^{7J/7J}$ IHCs and OHCs (Fig. 2E and Supplementary Material, Table S2), indicating that myosin VIIa is likely the major motor protein that localizes PDZD7 at the ankle link region. Therefore, myosin VIIa could be involved in transporting USH2 proteins along the actin filaments in the cochlear hair cell cytoplasm and/or anchoring these proteins to the actin bundles at the stereociliary base. Interestingly, immunostaining of *Myo7a*$^{7J/7J}$ retinas did not show obvious mislocalization of whirlin (Supplementary Material, Fig. S2). Because we previously reported that the protein level of whirlin is normal in *Myo7a*$^{7J/7J}$ retinas (38) and that whirlin recruits ADGRV1 and usherin to the periciliary membrane complex in photoreceptors (39), this result indicates that the localization of ADGRV1 and usherin in *Myo7a*$^{7J/7J}$ photoreceptors is probably normal. Therefore, the role of myosin VIIa in USH2 complex assembly is not the same in hair cells and photoreceptors.

USH1G interacts with the cytoplasmic region of ADGRV1 and usherin in vitro, but is dispensable for the normal localization of USH2 proteins in cochlear hair cells

USH1G (also known as SANS) interacts directly with whirlin through the whirlin PDZ1 and PDZ2 domains (30) and also interacts with PDZD7 (33) *in vitro*. In this study, we investigated whether USH1G interacted with ADGRV1 and usherin. USH1G is a cytoplasmic protein; therefore, its interactions with ADGRV1 and usherin would occur inside cells. We thus cotransfected HEK293 cells with FLAG-tagged ADGRV1 or usherin cytoplasmic fragment and GFP-tagged full-length USH1G. FLAG pull-down assays (Fig. 3A) showed that FLAG-ADGRV1 and FLAG-usherin cytoplasmic fragments were able to pull down GFP-USH1G but not GFP. Additionally, FLAG tag was unable to pull down GFP. These results indicated that USH1G interacts specifically with ADGRV1 and usherin cytoplasmic fragments. However, USH1G was previously reported to colocalize only partially with whirlin when cotransfected in COS7 cells and not to colocalize with USH2 proteins in cochlear hair cells (15,24,40). To test the possibility that USH1G associated with USH2 proteins transiently during the transport of USH2 proteins to the ankle link region and thus played a role in the localization of the USH2 complex in cochlear hair cells, we performed immunostaining of *Ush1g*$^{is\text{-}2J}$ (referred to hereafter as *Ush1g*$^{2J/2J}$) cochleas for USH2 proteins.

We first identified the *Ush1g*$^{2J/2J}$ mutation as c.302_456del (NM_176847) using the mouse genomic DNA by PCR and DNA sequencing (not shown). At the protein level, this mutation (p.Leu81GlyfsTer103) led to a protein fragment truncated before any predicted USH1G functional domains. Therefore, the *Ush1g*$^{2J/2J}$ mouse was *Ush1g*-null. In *Ush1g*$^{2J/2J}$ mice at P4, the stereocilia were severely splayed and disorganized in the stereociliary bundle, similar to those reported in *Ush1g*^{is} mice, a different *Ush1g* mutant mouse line (35). Among the stereociliary bundles in the entire *Ush1g*$^{2J/2J}$ cochlea, we chose the ones less disorganized to examine USH2 protein localization (Fig. 3B–D). ADGRV1 (Fig. 3B) and usherin (Fig. 3C) remained at the base of stereocilia, similar to wild-type mice (Fig. 2A). Whirlin was localized normally at both the tip and the base of the stereocilia (Fig. 3D). The percentages of *Ush1g*$^{2J/2J}$ IHCs and OHCs with abnormal ADGRV1, usherin or whirlin distribution were very low and are shown in Supplementary Material, Table S2. We previously showed that PDZD7 was normally localized in the cochlear stereociliary bundle of *Ush1g*$^{2J/2J}$ mice (16). Therefore, unlike myosin VIIa, despite the *in vitro* interaction of USH1G with each of the USH2 proteins, USH1G is dispensable for the localization of the USH2 complex in cochlear hair cells.

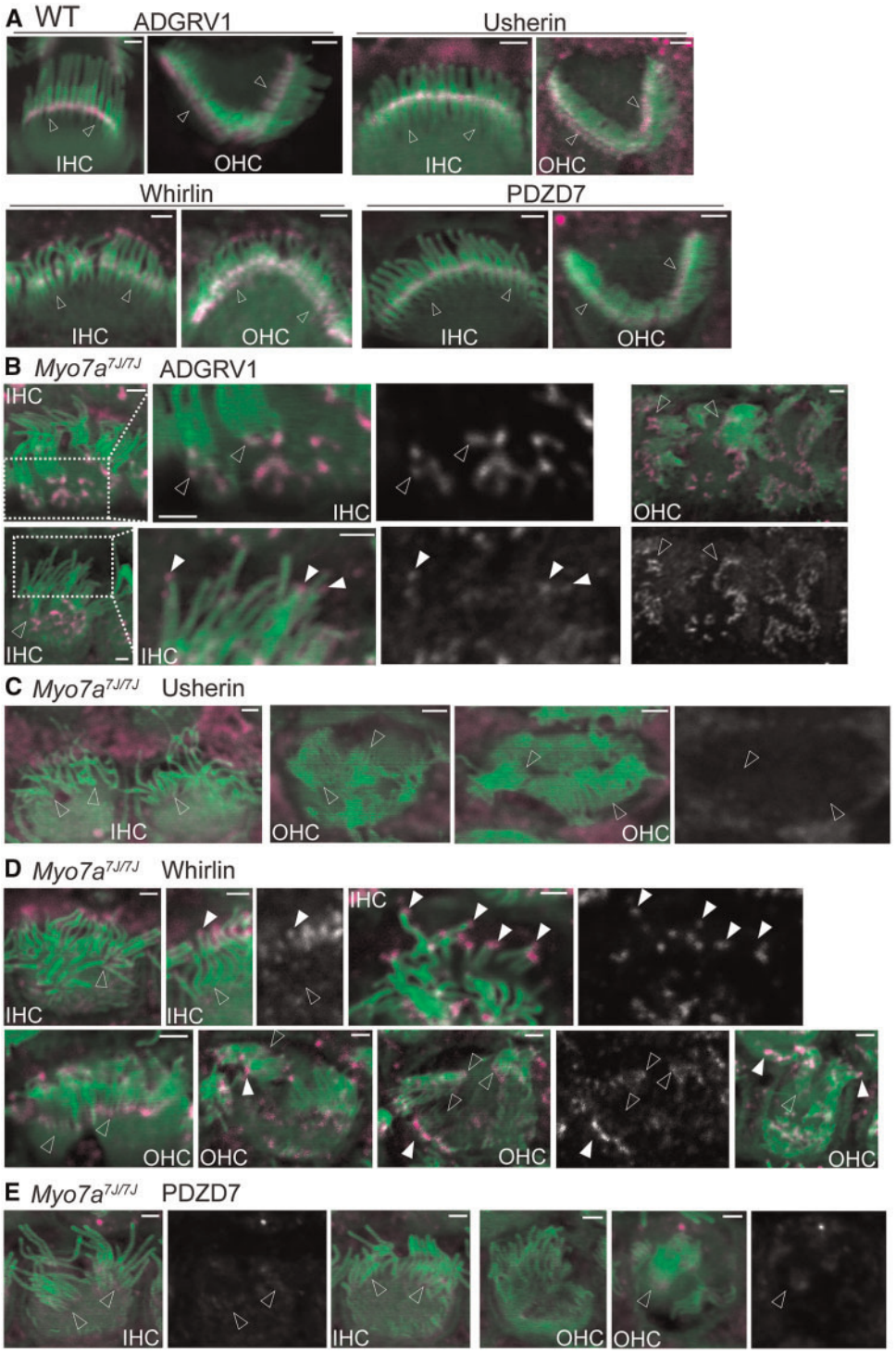

Figure 2. USH2 protein distribution is abnormal in *Myo7a*$^{7J/7J}$ cochlear hair cells. (**A**) USH2 protein distribution in wild-type (WT) cochlear IHCs and OHCs at P4. ADGRV1, usherin, whirlin and PDZD7 (magenta) are localized to the ankle link region at the base (empty arrows) of stereocilia (phalloidin, green), while whirlin is also present at the stereociliary tip. The immunoreactive specificity of our USH2 antibodies in these stereociliary locations was previously verified by absence of their immunoreactivities in their corresponding mutant cochlear stereociliary bundles (15). Note that the magenta signals outside the stereociliary bundle are non-specific. For an unknown reason, our usherin antibody usually gave this non-specific signal. (**B**) In P4 *Myo7a*$^{7J/7J}$ IHCs and OHCs, a large amount of ADGRV1 forms aggregates at the medial side of the stereociliary bundle on the apical surface of hair cells, while a trace amount of ADGRV1 remains at the ankle links (empty arrows) and is mislocalized at the stereociliary tips (filled arrows). The signal intensity at the stereociliary tip was ~10% of those at the stereociliary base and at the cell apex and was thus enhanced in order to be seen. Boxed regions are amplified and shown on the right of the original images. $n \geq 2$ pups from 1 litter. (**C**) Usherin immunofluorescence is undetectable in P4 *Myo7a*$^{7J/7J}$ IHCs and OHCs. Empty arrows: the base of stereocilia. $n \geq 3$ pups from 3 litters. (**D**) Immunofluorescent signals of whirlin are detectable at the tip (filled arrows) but not at some of the ankle link region (empty arrows) in P4 *Myo7a*$^{7J/7J}$ cochlear stereociliary bundles. $n \geq 3$ pups from 3 litters. (**E**) Immunoreactivity of PDZD7 is barely detectable at the stereociliary base (empty arrows) of P4 *Myo7a*$^{7J/7J}$ IHCs and OHCs. $n \geq 2$ pups from 1 litter. Some single-channel images of USH2 proteins are shown in grayscale on the right of or below the merged images, where the position of arrows is matched in the single-channel and merged images. Scale bars, 1 μm.

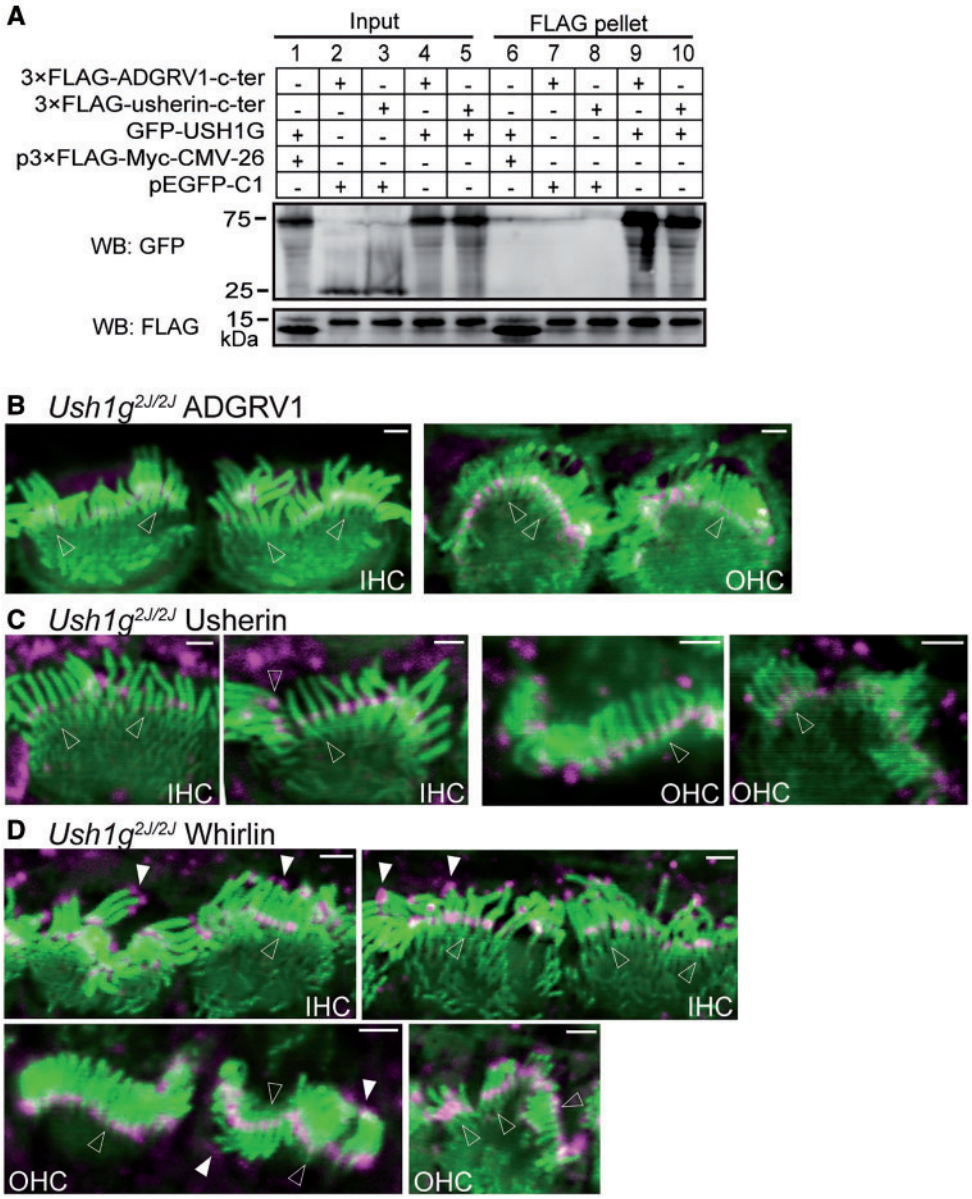

Figure 3. Interactions of USH1G with usherin and ADGRV1 and distribution of USH2 proteins in *Ush1g*$^{2J/2J}$ cochlear hair cells. (**A**) GFP-USH1G (lane 9 and lane 10), but not GFP (pEGFP-C1, lane 7 and lane 8), was pulled down by FLAG-usherin and FLAG-ADGRV1 cytoplasmic fragments (c-ter) using anti-FLAG M2 affinity agarose. The FLAG peptide expressed by p3xFLAG-Myc-CMV-26 vector was used as a negative control (lane 6). The bottom anti-FLAG blot demonstrates the success of the FLAG pull-down assay. Lanes 1-5 are input samples showing the expression of GFP-USH1G, GFP, FLAG-usherin c-ter, FLAG-ADGRV1 c-ter and FLAG peptide in the transfected HEK293 cells. + and -, presence and absence of protein fragments in the transfected cells, respectively. (**B**-**D**) Although the stereociliary bundle (phalloidin, green) is significantly distorted in *Ush1g*$^{2J/2J}$cochlear hair cells, localizations of ADGRV1 (magenta, **B**), usherin (magenta, **C**) and whirlin (magenta, **D**) at the ankle link region (empty arrows) are normal. Additionally, whirlin localization at the stereociliary tips (filled arrows, **D**) is also normal in P4 *Ush1g*$^{2J/2J}$cochlear hair cells. $n \geq 2$ pups from 2 litters for ADGRV1 immunostaining; $n \geq 4$ pups from 4 litters for usherin immunostaining; and $n \geq 2$ pups from 2 litters for whirlin immunostaining. The magenta signals outside the stereociliary bundle are non-specific. Scale bars, 1 μm.

CIB2 plays an insignificant role in the localization of Ush2 proteins in cochlear hair cells

CIB2 was recently identified as the causative gene for USH1J and nonsyndromic autosomal recessive deafness DFNB48 (32). Its protein CIB2 was previously reported to interact with whirlin *in vitro* (32). Therefore, we studied whether CIB2 was important for the localization of USH2 proteins in cochlear hair cells during development. Unlike other USH1 proteins that have been extensively studied in various mouse models, CIB2 has been studied mainly in zebrafish and drosophila by morpholino and RNA interference-mediated knockdown, respectively (32). We generated *Cib2*^{tm1} mice (referred to as *Cib2*$^{-/-}$ mice thereafter), in which a gene trap cassette was inserted between exon 3 and exon 4 of the *Cib2* gene (Supplementary Material, Fig. S3) and is expected to affect the expression of all four *Cib2* splice variants. We tested the hearing function of *Cib2*$^{-/-}$ mice to examine whether the *Cib2*$^{-/-}$ mice exhibit hearing impairment similar to that observed in USH1J and DFNB48 patients as well as in *cib2* knockdown zebrafish (32). Auditory brainstem response (ABR) tests found that the response thresholds of *Cib2*$^{-/-}$ mice to

sounds at 4–45 kHz were significantly elevated at P35 (Fig. 4A). Therefore, *Cib2*$^{-/-}$ mice had profound hearing loss. Distortion product otoacoustic emission (DPOAE) tests at the same age also showed significantly high thresholds in *Cib2*$^{-/-}$ mice at the f_2 frequencies of 8–32 kHz (Fig. 4B), indicating that the cochlear OHCs were dysfunctional in *Cib2*$^{-/-}$ mice. We further assessed the balance behaviour of *Cib2*$^{-/-}$ mice at P40 by rotarod tests. To our surprise, although *Cib2*$^{-/-}$ mice did not show obvious circling or head bobbing behaviour, they were unable to stay on the rotating rod as long as their wild-type littermates (Fig. 4C), indicating that the vestibular system, probably the utricle and saccule, of *Cib2*$^{-/-}$ mice might have defects.

Phalloidin staining of *Cib2*$^{-/-}$ cochleas at P4 showed that the morphology of *Cib2*$^{-/-}$ stereociliary bundles was grossly normal with three rows of stereocilia (Fig. 5), unlike the stereociliary bundles in other USH1 mutant cochleas, which were usually split into several tufts (*e.g.* Fig. 2B,D,E, 3C and D, 5C and D) (35). The planar cellular polarity of the stereociliary bundles in *Cib2*$^{-/-}$ cochleas also appeared normal. Because of the low resolution of phalloidin staining compared with scanning electron microscopy, we did not measure the length and width of individual stereocilia. The most obvious abnormality in *Cib2*$^{-/-}$ cochlear hair cells at P4 was the small ectopic stereocilia extending from the bundle toward the medial side on the OHC apexes (1.9% from 1569 wild-type cells, $n \geq 14$ pups; 29.2% from 349 *Cib2*$^{-/-}$ cells, $n \geq 8$ pups, blue arrows in Fig. 5A,C and D). Occasionally, ectopic stereocilia were also observed on the IHC apex (6.1% from 556 wild-type cells, $n \geq 14$ pups; 16.7% from 114 *Cib2*$^{-/-}$ cells, $n \geq 8$ pups, red arrow in Fig. 5A). Despite these defects, immunostaining of *Cib2*$^{-/-}$ cochleas at P4 demonstrated that ADGRV1 (Fig. 5A), usherin (Fig. 5B), whirlin (Fig. 5C) and PDZD7 (Fig. 5D) were normally localized at the base of stereocilia, with whirlin also normally located at stereociliary tips (Fig. 5D) in all IHCs and OHCs examined (Supplementary Material, Table S2). These findings suggest that CIB2 is not necessary for USH2 protein localizations in cochlear stereociliary bundles and CIB2 protein may not interact with USH2 proteins *in vivo*.

Harmonin, a PDZ domain-containing Ush1 protein, is not essential for localization of the Ush2 protein complex in cochlear hair cells

Among all USH1 proteins, harmonin, encoded by the *USH1C* gene, is paralogous to the two scaffold proteins in the USH2 complex, whirlin and PDZD7 (12,33). Despite the existence of alternative splicing in the genes encoding these three proteins, their long isoforms all have three PDZ domains, a proline-rich region and several harmonin N-like domains (14,28). The PDZ1 domain of the harmonin a1 splicing isoform, similar to the PDZ1 and PDZ2 domains of whirlin and PDZD7 (12,14,41), interacts directly with the PDZ-binding motif of ADGRV1 and usherin (31). Additionally, harmonin a1 was shown to associate with PDZD7 in the mouse retinal lysate (33). Based on these findings, we studied whether harmonin was important for USH2 complex localization at the ankle link region during cochlear hair cell development. We performed immunostaining for each USH2 protein at P4 in *Ush1c*$^{-/-}$ mice (42). Because *Ush1c*$^{-/-}$ stereociliary bundles were usually splayed and divided into multiple stereociliary tufts (42), examination of USH2 protein localization was conducted in the stereociliary bundles with a relatively better morphology. ADGRV1, usherin and PDZD7 were present at the stereociliary bases, and whirlin was present at both the stereociliary tips and bases in all *Ush1c*$^{-/-}$ IHCs and OHCs examined (Fig. 6 and Supplementary Material, Table S2). The USH2 protein

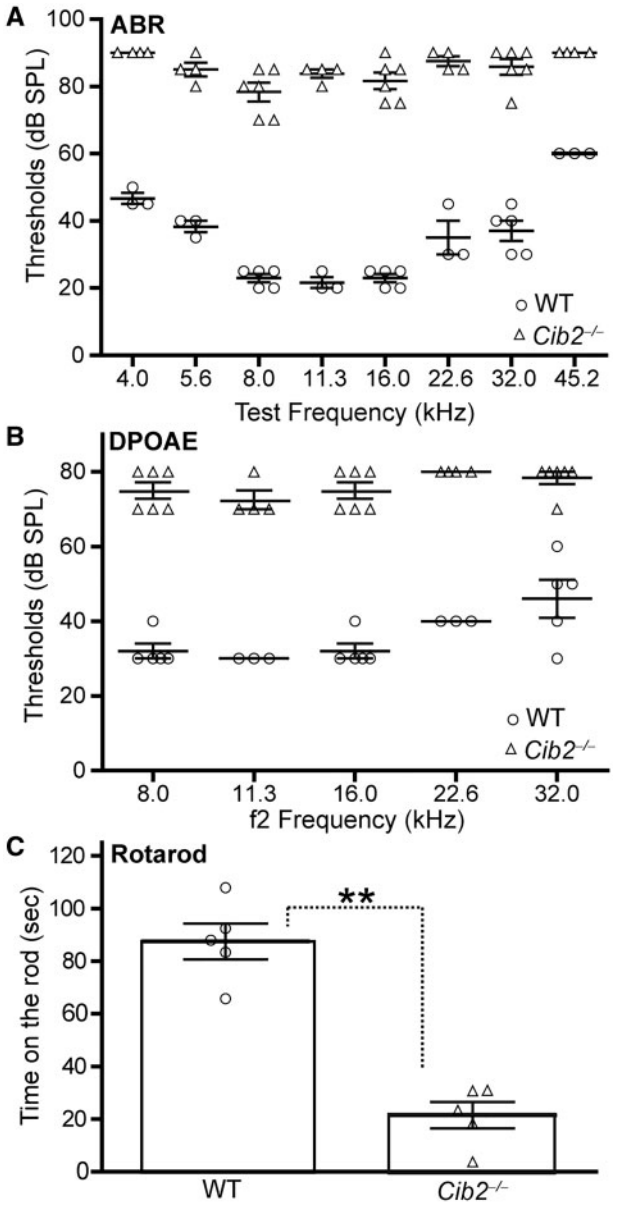

Figure 4. Hearing and balance impairments in *Cib2*$^{-/-}$ mice. ABR (**A**) and DPOAE (**B**) thresholds in *Cib2*$^{+/+}$ (WT) and *Cib2*$^{-/-}$ littermates at P35. $n = 3$-5 mice for WT and $n = 4$–6 mice for *Cib2*$^{-/-}$. Error bars, standard error of the mean (SEM). $P < 0.01$ when thresholds were compared between *Cib2*$^{+/+}$ and *Cib2*$^{-/-}$ littermates at each sound frequency. (**C**) Rotarod result of *Cib2*$^{+/+}$ and *Cib2*$^{-/-}$ littermates at P40. $n = 5$ mice for each group. Error bars, SEM. $^{**}P < 0.01$.

distributions in *Ush1c*$^{-/-}$ cochleas were indistinguishable from those in wild-type cochleas (Fig. 2A). Therefore, although harmonin is a close paralog of whirlin and PDZD7 and is localized in cochlear stereociliary bundles, harmonin is not involved in the localization of the USH2 complex in cochlear hair cells.

The PDZ domain-containing USH2 proteins, whirlin and PDZD7, play a synergistic role in usherin localization in cochlear hair cells

We previously reported that the two paralogs of harmonin, PDZD7 and whirlin, are both required to interact with ADGRV1 and usherin to form the USH2 quaternary protein complex (14). In cochlear

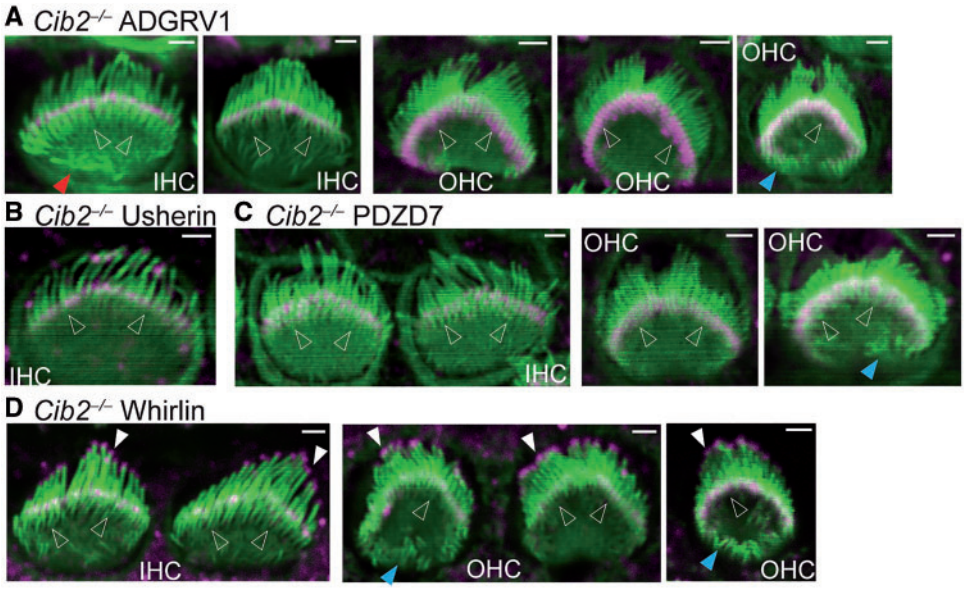

Figure 5. Normal distribution of USH2 proteins in *Cib2*$^{-/-}$ cochlear hair cells. Immunofluorescent staining demonstrated that ADGRV1 (magenta, **A**), usherin (magenta, **B**), PDZD7 (magenta, **C**) and whirlin (magenta, **D**) are localized at the base (empty arrows) of stereocilia (phalloidin, green), while whirlin is also localized at the stereociliary tips (white filled arrows) in P4 *Cib2*$^{-/-}$ cochlear hair cells. Blue and red arrows point to the ectopic stereocilia found in *Cib2*$^{-/-}$ OHCs and IHCs, respectively. Experiments were performed in 3 litters of *Cib2*$^{-/-}$ pups for ADGRV1 immunostaining, 1 litter for usherin immunostaining, 1 litter for PDZD7 immunostaining and 2 litters for whirlin immunostaining. Scale bars, 1 μm.

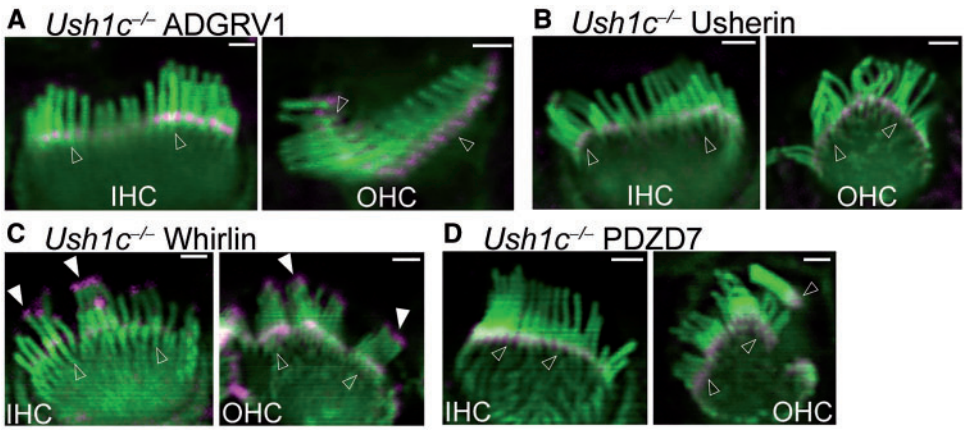

Figure 6. USH2 protein distribution is normal in *Ush1c*$^{-/-}$ cochlear hair cells. Immunofluorescent staining of *Ush1c*$^{-/-}$ cochleas at P4 demonstrated that ADGRV1 (magenta, **A**), usherin (magenta, **B**), whirlin (magenta, **C**) and PDZD7 (magenta, **D**) are localized at the base (empty arrows) of stereocilia (phalloidin, green) in IHCs and OHCs, while whirlin is also localized at the stereociliary tip (filled arrows) in IHCs and OHCs. The experiments were performed in 2 litters of *Ush1c*$^{-/-}$ pups for ADGRV1 immunostaining, 1 litter for usherin immunostaining, 4 litters for whirlin immunostaining and 2 litters for PDZD7 immunostaining. Scale bars, 1 μm.

hair cells, PDZD7 is essential for the localization of ADGRV1, usherin and whirlin, while whirlin plays only a minor role in the localization of ADGRV1 and is not involved in the localization of usherin or PDZD7 (15,16). We here studied whether PDZD7 and whirlin functioned synergistically in localizing ADGRV1 and usherin in cochlear hair cells during development. We generated *Pdzd7*$^{-/-}$;*Whrn*$^{neo/neo}$ double-mutant mice. Immunostaining found that usherin immunoreactivity was absent in the IHCs (100%) and nearly indiscernible in the OHCs (~99%) of *Pdzd7*$^{-/-}$;*Whrn*$^{neo/neo}$ mice at P4 (Fig. 7C and Supplementary Material, Table S3). Consistent with our previous reports (15,16), usherin was significantly reduced in the ankle link region of IHCs (~67%) and was localized diffusely along stereocilia of OHCs (~87%) in P4 *Pdzd7*$^{-/-}$ cochleas (Fig. 7B and Supplementary Material, Table S3), and usherin was localized almost normally at the base of stereocilia in P4 *Whrn*$^{neo/neo}$ IHCs (~97%) and OHCs (~99%) (Fig. 7A and Supplementary Material, Table S3). Therefore, PDZD7 and whirlin probably have a synergistic effect on normal usherin localization in cochlear hair cells. Immunostaining also showed that the mislocalized ADGRV1 signals had a similar pattern in *Pdzd7*$^{-/-}$;*Whrn*$^{neo/neo}$ and *Pdzd7*$^{-/-}$ cochlear hair cells at P4 (Fig. 8B and C). Both showed random punctate signals along the stereocilia or at the stereociliary tip. These defective ADGRV1 signal patterns were observed in all the examined IHCs and OHCs of *Pdzd7*$^{-/-}$;*Whrn*$^{neo/neo}$ and *Pdzd7*$^{-/-}$ mice (Supplementary Material, Table S3). In most *Whrn*$^{neo/neo}$ cochlear stereociliary bundles (~63% for IHCs and ~68% for OHCs), ADGRV1 distribution was normal, while a small amount of ADGRV1 was mislocalized at the stereociliary tip in the rest of *Whrn*$^{neo/neo}$ hair cells (Fig. 8A and Supplementary Material, Table S3). We further tested the hearing function of *Pdzd7*$^{-/-}$;*Whrn*$^{neo/neo}$ mice by ABR and

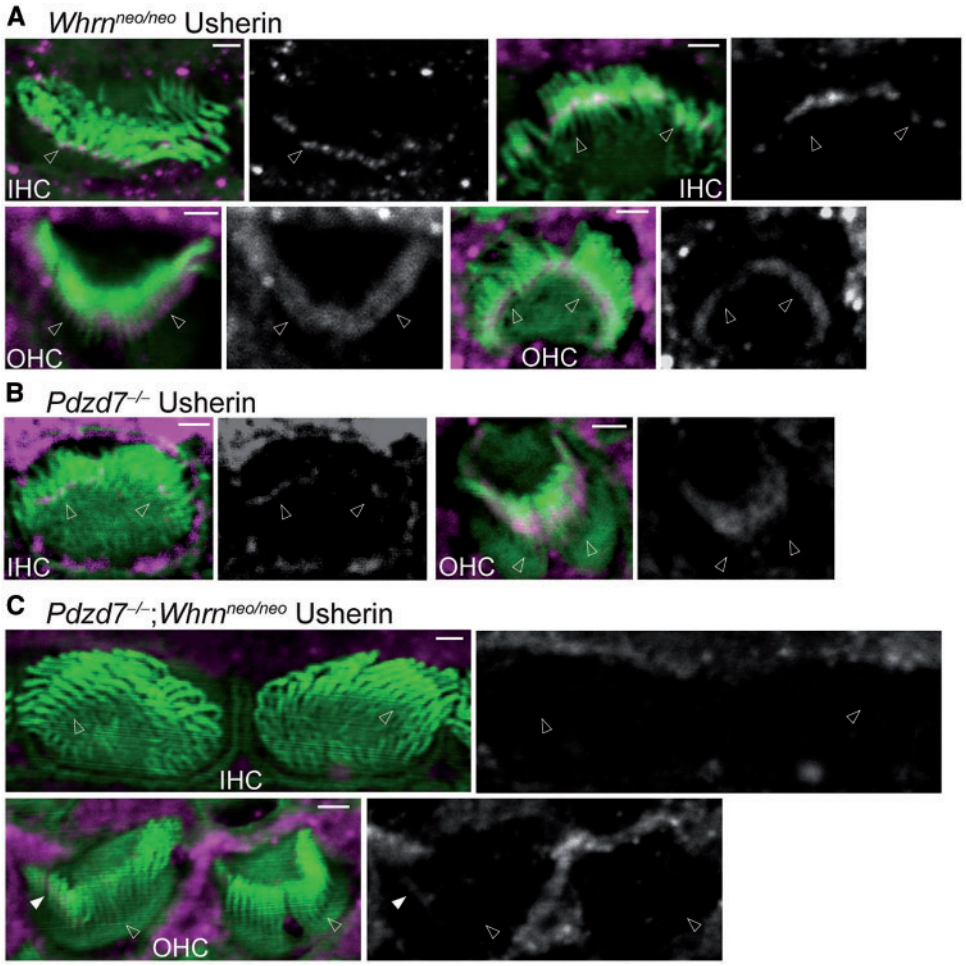

Figure 7. Usherin is undetectable at the ankle link region in the *Pdzd7*$^{-/-}$;*Whrn*$^{neo/neo}$ cochlear stereociliary bundle. (**A**) Usherin (magenta) is normally localized at the base of stereocilia (phalloidin, green) in P4 *Whrn*$^{neo/neo}$ IHCs and OHCs. $n \geq 3$ pups from 3 litters. (**B**) Usherin is reduced at the stereociliary base of *Pdzd7*$^{-/-}$ IHCs and moves toward stereociliary tips in *Pdzd7*$^{-/-}$ OHCs at P4. Usherin signal was enhanced in the IHC to show the reduced signal at the stereociliary base. $n \geq 3$ pups from 3 litters. (**C**) Usherin immunoreactivity is absent in the IHC stereociliary bundle and is barely detectable in the OHC stereociliary bundle in P4 *Pdzd7*$^{-/-}$;*Whrn*$^{neo/neo}$ cochleas. The filled arrow points to an extremely weak and diffuse usherin signal in the middle of stereocilia. $n \geq 2$ pups from 2 litters. The magenta signals outside the stereociliary bundle in this figure are non-specific and were usually seen for usherin staining. Single-channel images of usherin signals are shown in grayscale on the right of the merged images with the position of arrows the same as that in the merged images. Empty arrows point to the base of stereocilia. Scale bars: 1 μm.

DPOAE at P45 (Fig. 9). The ABR thresholds were similar between *Pdzd7*$^{-/-}$;*Whrn*$^{neo/neo}$ and *Pdzd7*$^{-/-}$ mice at the sound frequencies from 4 to 45 kHz, except at 11.3 kHz where the *Pdzd7*$^{-/-}$;*Whrn*$^{neo/neo}$ mice had a threshold that was approximately 10% higher than *Pdzd7*$^{-/-}$ mice ($P < 0.05$). DPOAE testing showed no difference in the thresholds between *Pdzd7*$^{-/-}$;*Whrn*$^{neo/neo}$ and *Pdzd7*$^{-/-}$ mice at the f_2 frequencies of 8–32 kHz. The ABR and DPOAE thresholds of *Pdzd7*$^{-/-}$;*Whrn*$^{neo/neo}$ and *Pdzd7*$^{-/-}$ mice were higher than those of *Whrn*$^{neo/neo}$ mice (40). Therefore, PDZD7 and whirlin act synergistically in usherin localization, but do not appear to act synergistically in ADGRV1 localization and hearing function.

Discussion

This study is the first to thoroughly examine the role of USH1 proteins in the assembly of the USH2 complex at ankle links in cochlear hair cells, multiprotein complex critical for a stereociliary bundle organization during development. We demonstrated that myosin VIIa, associated with USH subtype 1B, is indispensable for normal localization of USH2 proteins and thus USH2 complex assembly in cochlear hair cells. This finding indicates a functional interaction between myosin VIIa and USH2 proteins in cochlear hair cells and an overlap between the molecular mechanisms underlying USH1B and USH2 pathogenesis. However, myosin VIIa plays an insignificant role in the USH2 complex assembly in retinal photoreceptors, supporting the notion that USH2 complex assembly is not exactly the same between cochlear hair cells and retinal photoreceptors. Additionally, although other USH1 proteins interact with USH2 proteins *in vitro*, we found that these USH1 proteins did not appear to function in USH2 complex assembly *in vivo*, as demonstrated by normal localization of USH2 proteins in the cochlear hair cells of the mutant mice lacking these USH1 proteins. These findings suggest that the previously reported *in vitro* interactions between USH1 and USH2 proteins (31) unlikely occur at the stereociliary base in cochlear hair cells. Finally, our study on the three paralogous PDZ domain-containing USH proteins, the USH1 protein harmonin and the two USH2 proteins PDZD7 and whirlin, showed that PDZD7 and whirlin function synergistically in USH2 complex assembly, while harmonin is not involved in this process in cochlear hair cells.

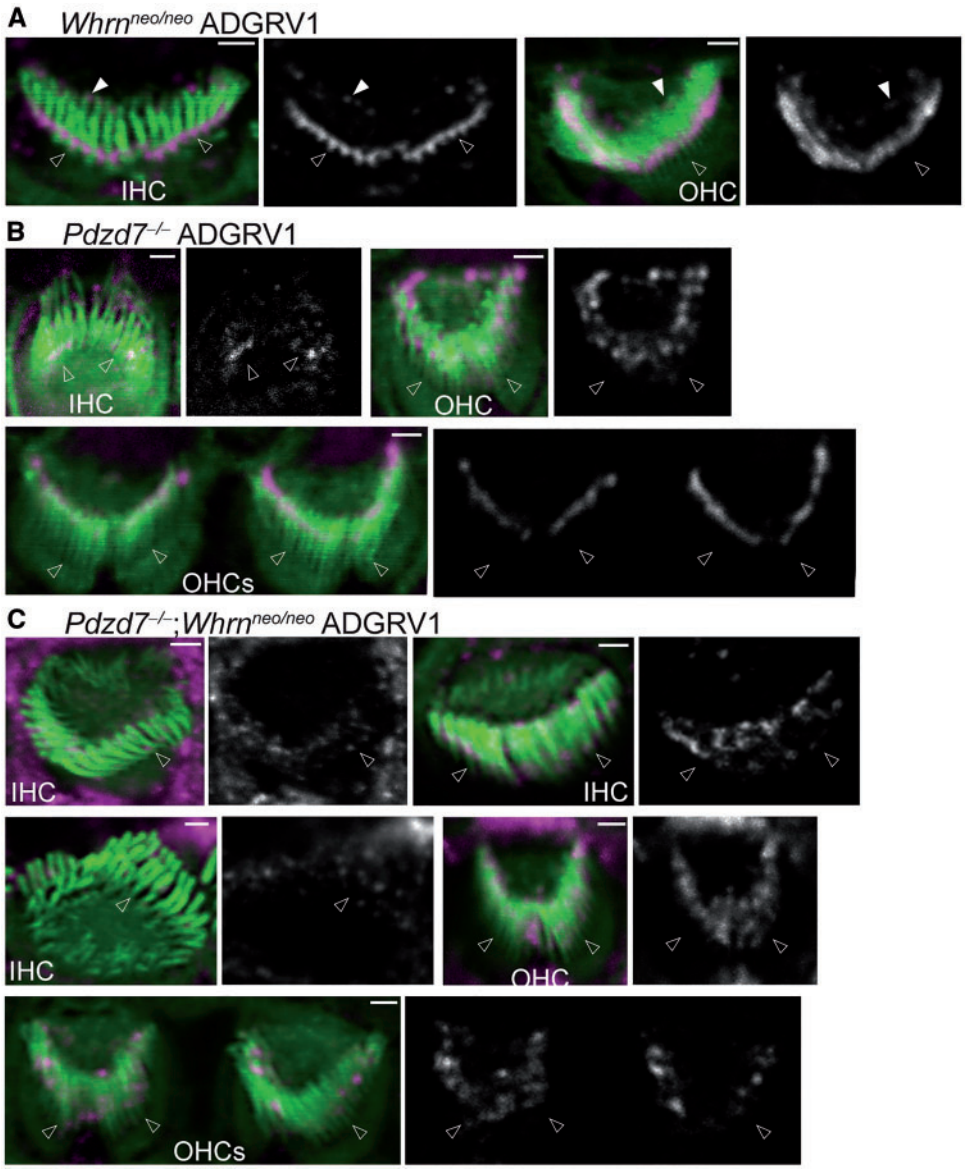

Figure 8. ADGRV1 mislocalization is similar between *Pdzd7*$^{-/-}$;*Whrn*$^{neo/neo}$ and *Pdzd7*$^{-/-}$ cochlear hair cells. (**A**) A small amount of ADGRV1 is mislocalized at the stereociliary tip (filled arrows) in about one third of *Whrn*$^{neo/neo}$ IHCs and OHCs. (**B**) ADGRV1 is localized either at the stereociliary tips or along the stereocilia as random puncta in *Pdzd7*$^{-/-}$ IHCs and OHCs. (**C**) In *Pdzd7*$^{-/-}$;*Whrn*$^{neo/neo}$ IHCs and OHCs, the severity and pattern of ADGRV1 mislocalization are similar to those observed in *Pdzd7*$^{-/-}$ IHCs and OHCs. One litter of *Whrn*$^{neo/neo}$ pups, one litter of *Pdzd7*$^{-/-}$ pups and five litters of *Pdzd7*$^{-/-}$;*Whrn*$^{neo/neo}$ pups were examined. The magenta signals outside the stereociliary bundle are non-specific. Single-channel images of ADGRV1 signals are shown in grayscale on the right of the merged images with the position of arrows the same as that in the merged images. Empty arrows, the base of stereocilia. Scale bars, 1 μm.

The functional significance of myosin VIIa in the USH2 complex could extend to all USH2 complex components, although these components have not yet been identified completely. Vezatin, an integral membrane protein, interacts with usherin and myosin VIIa *in vitro* (43) and transiently colocalizes with ADGRV1 at ankle links during stereociliary bundle development (13). Vezatin is thus thought to be a component of the USH2 complex in hair cells. In *Myo7a*^{4626SB} mutant mice, the distribution of vezatin at the stereociliary base is perturbed (13). Additionally, myosin VIIa partially overlaps USH1 proteins at distinct stereociliary positions (24,25,32,44–49), since myosin VIIa is localized along the entire stereocilia during mammalian cochlear development (23,35,50,51). Myosin VIIa interacts *in vitro* with USH1 proteins including CDH23, PCDH15, harmonin and USH1G (23,24,51,52) and is essential for harmonin and PCDH15 localization in stereociliary bundles (35,51,53). Therefore, myosin VIIa is likely a linker between the USH1 and USH2 complexes at the stereociliary bundle in hair cells. Myosin VIIa is an actin-based motor protein with a slow ADP releasing rate and a long lifetime binding to actin filaments (54). In cochlear hair cells, myosin VIIa may take part in transporting USH1 and USH2 proteins from the cell body to the stereociliary bundle and/or tethering USH1 and USH2 proteins to actin filaments in the stereociliary bundle. These two potential functions of myosin VIIa could exist simultaneously or one could be more predominant than the other.

Harmonin is localized at the stereociliary tip during embryonic development and moves to the UTLD during postnatal development in mouse cochleas (23–25,35). At the UTLD, harmonin is involved in mechanotransduction through

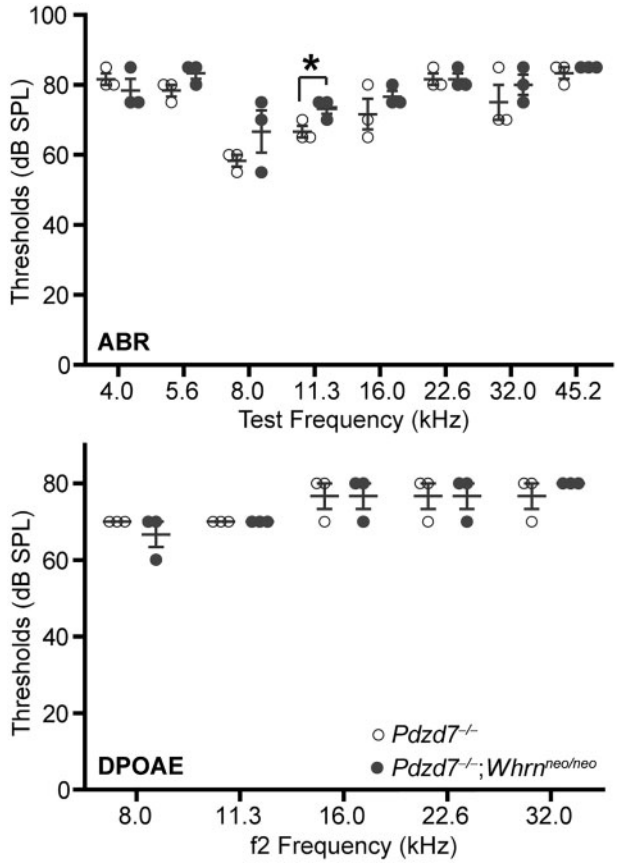

Figure 9. The severity of hearing loss is similar between *Pdzd7*$^{-/-}$;*Whrn*$^{neo/neo}$ and *Pdzd7*$^{-/-}$ mice. The ABR and DPOAE thresholds are elevated to similar levels in *Pdzd7*$^{-/-}$;*Whrn*$^{neo/neo}$ and *Pdzd7*$^{-/-}$ mice at P45. $n = 3$ mice for each group. *$P < 0.05$. Error bars, SEM.

interactions with CDH23, myosin VIIa and USH1G (23–25). The overt cochlear phenotypes in *Ush1c* (24,25,35), *Pdzd7* (16) and *Whrn* (21,40,55,56) single-mutant mice suggest that harmonin, PDZD7 and whirlin have their own distinct functions in the cochlear stereociliary bundle and are unable to completely compensate for each other's loss. Our present study clearly demonstrated that harmonin does not participate in the assembly of the USH2 complex. We showed that the abnormal usherin localization in *Pdzd7*$^{-/-}$;*Whrn*$^{neo/neo}$ mice is much more severe than the sum of those in *Pdzd7*$^{-/-}$ and *Whrn*$^{neo/neo}$ mice, suggesting a synergistic effect between PDZD7 and whirlin functions. The similar severity of ADGRV1 mislocalization and ABR/DPOAE threshold elevations between *Pdzd7*$^{-/-}$;*Whrn*$^{neo/neo}$ mice and *Pdzd7*$^{-/-}$ mice is probably due to the dominant role of PDZD7 over whirlin in ADGRV1 localization as well as stereociliary bundle morphology and function (15). The similar ABR/DPOAE phenotypes between *Pdzd7*$^{-/-}$;*Whrn*$^{neo/neo}$ mice and *Pdzd7*$^{-/-}$ mice also suggest that the different degrees of defective usherin localization at the stereociliary bundle may contribute insignificantly to hearing loss.

In summary, our findings shed new light on the molecular mechanisms underlying stereociliary bundle development, which is crucial to understand the biology and mechanotransduction in cochlear hair cells. Furthermore, the findings in this study provide new clues to the disease mechanisms underlying hearing loss in both USH1 and USH2 and might be valuable for developing mechanism-based therapies in the future.

Materials and Methods

Animals

Cib2$^{tm1a(EUCOMM)Wtsi}$ (*Cib2*$^{-/-}$, MGI: 4432101) frozen sperms were purchased from the European Conditional Mouse Mutagenesis Program (EUCOMM) and revived by the University of Utah Transgenic and Gene Targeting Mouse Facility. *Myo7a*$^{sh1\text{-}7J}$/J (*Myo7a*$^{7J/7J}$, Jax stock # 002919, MGI: 3045593) and *Ush1g*$^{js\text{-}2J}$/J (*Ush1g*$^{2J/2J}$, Jax stock # 006111, MGI: 3640130) mice were purchased from the Jackson Laboratory (Bar Harbor, ME, USA). *Whrn*^{tm1Tili} (*Whrn*$^{neo/neo}$, MGI: 4462398), *Pdzd7*$^{tm1a(EUCOMM)Wtsi}$ (*Pdzd7*$^{-/-}$, MGI: 4433578) and *Ush1c*^{tm1Xzl} (*Ush1c*$^{-/-}$, MGI: 4437562) mice were generated as described previously (16,21,42). All experiments involving animals were approved by the Institutional Animal Care and Use Committee at the University of Utah.

RNA isolation, reverse transcription-polymerase chain reaction (RT-PCR) and DNA construct cloning

Total RNA was isolated from mouse retinas and inner ears using TRIzol reagent (Life Technologies, Carlsbad, CA, USA) and was used to generate cDNAs using oligo(dT) or random primers by ThermoScript™ RT-PCR system (Life Technologies, Carlsbad, CA, USA). Myosin VIIa tail cDNA (2799–6908 bp in NM_001256081 corresponding to 847–2215 aa in NP_001243010) was cloned into p3xFLAG-Myc-CMV-26 vector (Sigma-Aldrich, St. Louis, MO, USA) at the NotI and EcoRI sites, and USH1G full-length cDNA (66–1448 bp in NM_176847 corresponding to 2–461 aa in NP_789817) was cloned into pEGFP-C1 vector (Clontech Laboratories, Inc., Mountain View, CA, USA) at the BamHI and EcoRI sites using standard molecular cloning approach. The constructs of GFP-PDZD7 FL (2–1021 aa, NP_001182194), GFP-PDZD7 PDZ1 (84–164 aa, NP_001182194), GFP-PDZD7 PDZ2 (209–289 aa, NP_001182194), GFP-PDZD7 PDZ3 (856 - 944 aa, NP_001182194), FLAG-ADGRV1-c-ter (6149–6298 aa, NP_473394) and FLAG-usherin-c-ter (5044–5193 aa, NP_067383) were made and described previously (14).

Antibodies

Rabbit polyclonal antibodies against GFP (full-length), myosin VIIa (1–997 aa, NP_001243010), ADGRV1 (1212–2211 aa, NP_473394), usherin (5053–5193 aa, NP_067383), whirlin (721–800 aa) and PDZD7 (680–1021 aa, NP_001182194) were generated previously (15,16). The specificity of these antibodies was verified by the presence of immunoreactivity in wild-type cochlear hair cells and lack of immunoreactivity in cochlear hair cells of the corresponding mutant mice (USH protein antibodies) or by the presence of immunoreactivity in GFP-transfected HEK293 cells but absence of immunoreactivity in non-transfected HEK293 cells (GFP antibody). Alexa fluorochrome-conjugated phalloidin and secondary antibodies (Life Technologies, Carlsbad, CA, USA), monoclonal mouse antibody against FLAG (F1804, Sigma-Aldrich, St. Louis, MO, USA) and horse radish peroxidase-conjugated secondary antibodies (Jackson ImmunoResearch Laboratories, West Grove, PA, USA) were purchased commercially.

Immunofluorescence

Postnatal mouse cochleas were dissected and fixed in 4% formaldehyde/PBS for 40 min (myosin VIIa, usherin and whirlin immunostaining), 2 h (PDZD7 immunostaining) or overnight

(ADGRV1 immunostaining). The cochleas were then permeabilized by incubating in 0.5% Triton X-100/PBS for 5 min. Additional incubations of cochleas for usherin and whirlin immunostaining were performed in 50 mM NH_4Cl for 15 min and in Tween Tris-buffered saline (20 mM Tris pH 7.5, 150 mM NaCl and 0.1% Tween 20) for 10 min. Adult mouse eyes were enucleated, frozen immediately in Tissue-Tek® O.C.T. compound (Sakura Finetek USA Inc, Torrance, CA, USA) and sectioned at 10 μm. Retinal sections were fixed in 4% formaldehyde/PBS for 10 min and permeabilized in 0.2% Triton X-100/PBS for 5 min. Whole-mount cochleas and retinal sections were subsequently blocked in 5% goat serum/PBS for 1 h, incubated with primary antibodies in 5% goat serum/PBS at a 1:2000 dilution ratio at 4°C overnight, washed several times with PBS and incubated with Alexa Fluor® 594-conjugated goat anti-rabbit secondary antibody and Alexa Fluor® 488-conjugated phalloidin (cochleas only) in 5% goat serum/PBS for 1 h. After extensive washes with PBS, the stained cochleas and retinal sections were mounted on glass slides using Shandon™ Immu-Mount™ aqueous non-fluorescing mounting medium (Thermo Electron Corporation, Pittsburgh, PA, USA) and imaged using an Olympus FV1000 confocal laser scanning microscope. For each immunostaining experiment, wild-type or heterozygous mice were included as a positive control.

FLAG pull-down assay and immunoblotting analysis

HEK293 cells (ATCC, Manassas, VA, USA), grown in Dulbecco's Modified Eagle Medium supplemented with 10% fetal bovine serum, 100 units/ml penicillin and 100 μg/ml streptomycin, were double transfected with GFP-tagged and FLAG-tagged cDNA plasmids using PEI, according to the manufacturer's protocol (Polysciences, Inc, Warrington, PA, USA). Cells were harvested 24 hours after transfection and homogenized in lysis buffer (50 mM Tris-HCl, pH 8.0, 150 mM NaCl, 0.5% (v/v) Triton X-100, 5 mM EDTA, 1 X protease inhibitor and 1 mM DTT). After centrifugation at 21,000 X g for 10 min, the supernatants of cell lysates were incubated with anti-FLAG M2 agarose affinity gel (A2220, Sigma-Aldrich, St. Louis, MO, USA) for 2 h or overnight with gentle agitation. The agarose beads and their binding proteins were then spun down, washed four times with lysis buffer and boiled in Laemmli sample buffer for 5 min. Standard immunoblotting procedures were followed using mouse monoclonal anti-FLAG M2 antibody and rabbit GFP antibody (14).

Auditory brainstem response (ABR), distortion product otoacoustic emission (DPOAE) and rotarod tests

ABR and DPOAE tests were conducted as previously described (16). Briefly, mice were anaesthetized by intraperitoneal injection of ketamine (100 mg/kg) and xylazine (10 mg/kg). Body temperature was maintained at 37°C using a heating lamp. An electrostatic speaker (EC-1, Tucker-Davis Technology, Alachua, FL, USA) fitted with a 1.5-cm long polyethylene tube was placed abutting the ear canal through a small incision at the tragus. Stimuli for ABR were digitally generated in SigGenRP, processed by a RX6 real-time processor and passed through a PA5 attenuator prior to delivery to the speaker. Recording electrodes were placed under the skin at the vertex and mastoid, and a remote ground electrode was placed in the rump area. ABR responses were bandpass (100–3000 Hz) filtered, amplified, digitized and averaged with a RA16BA processor controlled by TDT BioSigRP software. ABR thresholds were determined as the lowest sound pressure levels (SPL) at which the response was clearly discernible.

DPOAEs were tested using an ER-10B± microphone (Etymotic Research, Elk Grove Village, IL, USA) coupled with two EC1 speakers. Stimuli of two primary tones f_1 *and* f_2 ($f_2/f_1 = 1.2$) were presented with $L_2 = L_1 - 10$ dB. Primary tones were stepped from 30 to 80 dB SPL (L_1) in 10 dB increments and swept from 8 to 32 kHz in ½ octave steps (f_2). Stimuli were generated and attenuated digitally (200 kHz sampling). The ear canal sound pressure was preamplified and digitized. A fast Fourier transformation was computed, and the sound pressures at f_1, f_2 and $2f_1 - f_2$ were extracted after spectral averaging from 50 serial waveform traces. DPOAE thresholds were determined as the lowest L_1 SPLs at which the $2f_1 - f_2$ distortion product was observable above the noise floor.

Rotarod testing was performed exactly as described previously (56).

Statistical analysis

Two-tailed Student's *t*-tests assuming equal variances were performed using Microsoft Office Excel. A *P*-value of < 0.05 was considered to indicate a significant difference between the values from two different groups.

Supplementary Material

Supplementary Material is available at *HMG* online.

Acknowledgements

We thank Ms. Susan Tamowski for assisting us in reviving the *Cib2*$^{-/-}$ mouse line at the University of Utah Transgenic and Gene Targeting Mouse Facility.

Conflict of Interest statement. None declared.

Funding

This work was supported by National Eye Institute [EY020853 to JY, EY014800 to the Department of Ophthalmology & Visual Sciences, University of Utah]; Research to Prevent Blindness, Inc. [to JY and the Department of Ophthalmology & Visual Sciences, University of Utah]; Knights Templar Eye Foundation [to QC]; Hearing Health Foundation [to JZ]; National Organization for Hearing Research Foundation [to JZ]; National Institute on Deafness and Other Communication Disorders [DC015111 to QYZ].

References

1. Boughman, J.A., Vernon, M. and Shaver, K.A. (1983) Usher syndrome: definition and estimate of prevalence from two high-risk populations. *J. Chronic Dis.*, **36**, 595–603.
2. Hartong, D.T., Berson, E.L. and Dryja, T.P. (2006) Retinitis pigmentosa. *Lancet*, **368**, 1795–1809.
3. Keats, B.J. and Corey, D.P. (1999) The usher syndromes. *Am. J. Med. Genet.*, **89**, 158–166.
4. Kimberling, W.J., Hildebrand, M.S., Shearer, A.E., Jensen, M.L., Halder, J.A., Trzupek, K., Cohn, E.S., Weleber, R.G., Stone, E.M. and Smith, R.J. (2010) Frequency of Usher syndrome in two pediatric populations: Implications for genetic

screening of deaf and hard of hearing children. *Genet. Med.*, **12**, 512–516.
5. Mathur, P. and Yang, J. (2015) Usher syndrome: hearing loss, retinal degeneration and associated abnormalities. *Biochim. Biophys. Acta*, **1852**, 406–420.
6. Assad, J.A., Shepherd, G.M. and Corey, D.P. (1991) Tip-link integrity and mechanical transduction in vertebrate hair cells. *Neuron*, **7**, 985–994.
7. Pickles, J.O., Comis, S.D. and Osborne, M.P. (1984) Cross-links between stereocilia in the guinea pig organ of Corti, and their possible relation to sensory transduction. *Hear. Res.*, **15**, 103–112.
8. Hudspeth, A.J. (1985) Models for mechanoelectrical transduction by hair cells. *Prog. Clin. Biol. Res.*, **176**, 193–205.
9. Ebermann, I., Scholl, H.P., Charbel Issa, P., Becirovic, E., Lamprecht, J., Jurklies, B., Millan, J.M., Aller, E., Mitter, D. and Bolz, H. (2007) A novel gene for Usher syndrome type 2: mutations in the long isoform of whirlin are associated with retinitis pigmentosa and sensorineural hearing loss. *Hum. Genet.*, **121**, 203–211.
10. Eudy, J.D., Weston, M.D., Yao, S., Hoover, D.M., Rehm, H.L., Ma-Edmonds, M., Yan, D., Ahmad, I., Cheng, J.J., Ayuso, C., *et al.* (1998) Mutation of a gene encoding a protein with extracellular matrix motifs in Usher syndrome type IIa. *Science*, **280**, 1753–1757.
11. Weston, M.D., Luijendijk, M.W., Humphrey, K.D., Moller, C. and Kimberling, W.J. (2004) Mutations in the VLGR1 gene implicate G-protein signaling in the pathogenesis of Usher syndrome type II. *Am. J. Hum. Genet.*, **74**, 357–366.
12. Ebermann, I., Phillips, J.B., Liebau, M.C., Koenekoop, R.K., Schermer, B., Lopez, I., Schafer, E., Roux, A.F., Dafinger, C., Bernd, A., *et al.* (2010) PDZD7 is a modifier of retinal disease and a contributor to digenic Usher syndrome. *J. Clin. Invest.*, **120**, 1812–1823.
13. Michalski, N., Michel, V., Bahloul, A., Lefevre, G., Barral, J., Yagi, H., Chardenoux, S., Weil, D., Martin, P., Hardelin, J.P., *et al.* (2007) Molecular characterization of the ankle-link complex in cochlear hair cells and its role in the hair bundle functioning. *J. Neurosci.*, **27**, 6478–6488.
14. Chen, Q., Zou, J., Shen, Z., Zhang, W. and Yang, J. (2014) Whirlin and PDZ domain containing 7 (PDZD7) proteins are both required to form the quaternary protein complex associated with Usher syndrome type 2. *J. Biol. Chem.*, **289**, 36070–36088.
15. Zou, J., Mathur, P.D., Zheng, T., Wang, Y., Almishaal, A., Park, A.H. and Yang, J. (2015) Individual USH2 proteins make distinct contributions to the ankle link complex during development of the mouse cochlear stereociliary bundle. *Hum. Mol. Genet.*, **24**, 6944–6957.
16. Zou, J., Zheng, T., Ren, C., Askew, C., Liu, X.P., Pan, B., Holt, J.R., Wang, Y. and Yang, J. (2014) Deletion of PDZD7 disrupts the Usher syndrome type 2 protein complex in cochlear hair cells and causes hearing loss in mice. *Hum. Mol. Genet.*, **23**, 2374–2390.
17. Goodyear, R.J., Marcotti, W., Kros, C.J. and Richardson, G.P. (2005) Development and properties of stereociliary link types in hair cells of the mouse cochlea. *J. Comp. Neurol.*, **485**, 75–85.
18. McGee, J., Goodyear, R.J., McMillan, D.R., Stauffer, E.A., Holt, J.R., Locke, K.G., Birch, D.G., Legan, P.K., White, P.C., Walsh, E.J., *et al.* (2006) The very large G-protein-coupled receptor VLGR1: a component of the ankle link complex required for the normal development of auditory hair bundles. *J. Neurosci.*, **26**, 6543–6553.
19. Liu, X., Bulgakov, O.V., Darrow, K.N., Pawlyk, B., Adamian, M., Liberman, M.C. and Li, T. (2007) Usherin is required for maintenance of retinal photoreceptors and normal development of cochlear hair cells. *Proc. Natl. Acad. Sci. U. S. A*, **104**, 4413–4418.
20. Mburu, P., Mustapha, M., Varela, A., Weil, D., El-Amraoui, A., Holme, R.H., Rump, A., Hardisty, R.E., Blanchard, S., Coimbra, R.S., *et al.* (2003) Defects in whirlin, a PDZ domain molecule involved in stereocilia elongation, cause deafness in the whirler mouse and families with DFNB31. *Nat. Genet.*, **34**, 421–428.
21. Yang, J., Liu, X., Zhao, Y., Adamian, M., Pawlyk, B., Sun, X., McMillan, D.R., Liberman, M.C. and Li, T. (2010) Ablation of whirlin long isoform disrupts the USH2 protein complex and causes vision and hearing loss. *PLoS Genet.*, **6**, e1000955.
22. Adato, A., Michel, V., Kikkawa, Y., Reiners, J., Alagramam, K.N., Weil, D., Yonekawa, H., Wolfrum, U., El-Amraoui, A. and Petit, C. (2005) Interactions in the network of Usher syndrome type 1 proteins. *Hum. Mol. Genet.*, **14**, 347–356.
23. Bahloul, A., Michel, V., Hardelin, J.P., Nouaille, S., Hoos, S., Houdusse, A., England, P. and Petit, C. (2010) Cadherin-23, myosin VIIa and harmonin, encoded by Usher syndrome type I genes, form a ternary complex and interact with membrane phospholipids. *Hum. Mol. Genet.*, **19**, 3557–3565.
24. Grati, M. and Kachar, B. (2011) Myosin VIIa and sans localization at stereocilia upper tip-link density implicates these Usher syndrome proteins in mechanotransduction. *Proc. Natl. Acad. Sci. U. S. A*, **108**, 11476–11481.
25. Grillet, N., Xiong, W., Reynolds, A., Kazmierczak, P., Sato, T., Lillo, C., Dumont, R.A., Hintermann, E., Sczaniecka, A., Schwander, M., *et al.* (2009) Harmonin mutations cause mechanotransduction defects in cochlear hair cells. *Neuron*, **62**, 375–387.
26. Pan, L., Yan, J., Wu, L. and Zhang, M. (2009) Assembling stable hair cell tip link complex via multidentate interactions between harmonin and cadherin 23. *Proc. Natl. Acad. Sci. U. S. A*, **106**, 5575–5580.
27. Wu, L., Pan, L., Wei, Z. and Zhang, M. (2011) Structure of MyTH4-FERM domains in myosin VIIa tail bound to cargo. *Science*, **331**, 757–760.
28. Yan, J., Pan, L., Chen, X., Wu, L. and Zhang, M. (2010) The structure of the harmonin/sans complex reveals an unexpected interaction mode of the two Usher syndrome proteins. *Proc. Natl. Acad. Sci. U. S. A*, **107**, 4040–4045.
29. Zheng, L., Zheng, J., Whitlon, D.S., Garcia-Anoveros, J. and Bartles, J.R. (2010) Targeting of the hair cell proteins cadherin 23, harmonin, myosin XVa, espin, and prestin in an epithelial cell model. *J. Neurosci.*, **30**, 7187–7201.
30. Maerker, T., van Wijk, E., Overlack, N., Kersten, F.F., McGee, J., Goldmann, T., Sehn, E., Roepman, R., Walsh, E.J., Kremer, H., *et al.* (2008) A novel Usher protein network at the periciliary reloading point between molecular transport machineries in vertebrate photoreceptor cells. *Hum. Mol. Genet.*, **17**, 71–86.
31. Reiners, J., van Wijk, E., Marker, T., Zimmermann, U., Jurgens, K., te Brinke, H., Overlack, N., Roepman, R., Knipper, M., Kremer, H., *et al.* (2005) Scaffold protein harmonin (USH1C) provides molecular links between Usher syndrome type 1 and type 2. *Hum. Mol. Genet.*, **14**, 3933–3943.
32. Riazuddin, S., Belyantseva, I.A., Giese, A.P., Lee, K., Indzhykulian, A.A., Nandamuri, S.P., Yousaf, R., Sinha, G.P., Lee, S., Terrell, D., *et al.* (2012) Alterations of the CIB2 calcium- and integrin-binding protein cause Usher syndrome

type 1J and nonsyndromic deafness DFNB48. *Nat. Genet.*, **44**, 1265–1271.
33. Schneider, E., Marker, T., Daser, A., Frey-Mahn, G., Beyer, V., Farcas, R., Schneider-Ratzke, B., Kohlschmidt, N., Grossmann, B., Bauss, K., *et al.* (2009) Homozygous disruption of PDZD7 by reciprocal translocation in a consanguineous family: a new member of the Usher syndrome protein interactome causing congenital hearing impairment. *Hum. Mol. Genet.*, **18**, 655–666.
34. Delprat, B., Michel, V., Goodyear, R., Yamasaki, Y., Michalski, N., El-Amraoui, A., Perfettini, I., Legrain, P., Richardson, G., Hardelin, J.P., *et al.* (2005) Myosin XVa and whirlin, two deafness gene products required for hair bundle growth, are located at the stereocilia tips and interact directly. *Hum. Mol. Genet.*, **14**, 401–410.
35. Lefevre, G., Michel, V., Weil, D., Lepelletier, L., Bizard, E., Wolfrum, U., Hardelin, J.P. and Petit, C. (2008) A core cochlear phenotype in USH1 mouse mutants implicates fibrous links of the hair bundle in its cohesion, orientation and differential growth. *Development*, **135**, 1427–1437.
36. Prosser, H.M., Rzadzinska, A.K., Steel, K.P. and Bradley, A. (2008) Mosaic complementation demonstrates a regulatory role for myosin VIIa in actin dynamics of stereocilia. *Mol. Cell. Biol.*, **28**, 1702–1712.
37. Grati, M., Shin, J.B., Weston, M.D., Green, J., Bhat, M.A., Gillespie, P.G. and Kachar, B. (2012) Localization of PDZD7 to the stereocilia ankle-link associates this scaffolding protein with the Usher syndrome protein network. *J. Neurosci.*, **32**, 14288–14293.
38. Yang, J., Wang, L., Song, H. and Sokolov, M. (2012) Current understanding of usher syndrome type II. *Front. Biosci.*, **17**, 1165–1183.
39. Zou, J., Luo, L., Shen, Z., Chiodo, V.A., Ambati, B.K., Hauswirth, W.W. and Yang, J. (2011) Whirlin replacement restores the formation of the USH2 protein complex in whirlin knockout photoreceptors. *Invest. Ophthalmol. Vis. Sci.*, **52**, 2343–2351.
40. Mathur, P., Zou, J., Zheng, T., Almishaal, A., Wang, Y., Chen, Q., Wang, L., Vashist, D., Brown, S., Park, A., *et al.* (2015) Distinct expression and function of whirlin isoforms in the inner ear and retina: an insight into pathogenesis of USH2D and DFNB31. *Hum. Mol. Genet.*, **24**, 6213–6228.
41. Adato, A., Lefevre, G., Delprat, B., Michel, V., Michalski, N., Chardenoux, S., Weil, D., El-Amraoui, A. and Petit, C. (2005) Usherin, the defective protein in Usher syndrome type IIA, is likely to be a component of interstereocilia ankle links in the inner ear sensory cells. *Hum. Mol. Genet.*, **14**, 3921–3932.
42. Tian, C., Liu, X.Z., Han, F., Yu, H., Longo-Guess, C., Yang, B., Lu, C., Yan, D. and Zheng, Q.Y. (2010) Ush1c gene expression levels in the ear and eye suggest different roles for Ush1c in neurosensory organs in a new Ush1c knockout mouse. *Brain Res.*, **1328**, 57–70.
43. Kussel-Andermann, P., El-Amraoui, A., Safieddine, S., Nouaille, S., Perfettini, I., Lecuit, M., Cossart, P., Wolfrum, U. and Petit, C. (2000) Vezatin, a novel transmembrane protein, bridges myosin VIIA to the cadherin-catenins complex. *Embo J.*, **19**, 6020–6029.
44. Ahmed, Z.M., Goodyear, R., Riazuddin, S., Lagziel, A., Legan, P.K., Behra, M., Burgess, S.M., Lilley, K.S., Wilcox, E.R., Griffith, A.J., *et al.* (2006) The tip-link antigen, a protein associated with the transduction complex of sensory hair cells, is protocadherin-15. *J. Neurosci.*, **26**, 7022–7034.
45. Kazmierczak, P., Sakaguchi, H., Tokita, J., Wilson-Kubalek, E.M., Milligan, R.A., Muller, U. and Kachar, B. (2007) Cadherin 23 and protocadherin 15 interact to form tip-link filaments in sensory hair cells. *Nature*, **449**, 87–91.
46. Michalski, N., Michel, V., Caberlotto, E., Lefevre, G.M., van Aken, A.F., Tinevez, J.Y., Bizard, E., Houbron, C., Weil, D., Hardelin, J.P., *et al.* (2009) Harmonin-b, an actin-binding scaffold protein, is involved in the adaptation of mechanoelectrical transduction by sensory hair cells. *Pflugers Arch.*, **459**, 115–130.
47. Michel, V., Goodyear, R.J., Weil, D., Marcotti, W., Perfettini, I., Wolfrum, U., Kros, C.J., Richardson, G.P. and Petit, C. (2005) Cadherin 23 is a component of the transient lateral links in the developing hair bundles of cochlear sensory cells. *Dev. Biol.*, **280**, 281–294.
48. Siemens, J., Lillo, C., Dumont, R.A., Reynolds, A., Williams, D.S., Gillespie, P.G. and Muller, U. (2004) Cadherin 23 is a component of the tip link in hair-cell stereocilia. *Nature*, **428**, 950–955.
49. Sollner, C., Rauch, G.J., Siemens, J., Geisler, R., Schuster, S.C., Muller, U. and Nicolson, T. (2004) Mutations in cadherin 23 affect tip links in zebrafish sensory hair cells. *Nature*, **428**, 955–959.
50. Hasson, T., Gillespie, P.G., Garcia, J.A., MacDonald, R.B., Zhao, Y., Yee, A.G., Mooseker, M.S. and Corey, D.P. (1997) Unconventional myosins in inner-ear sensory epithelia. *J. Cell Biol.*, **137**, 1287–1307.
51. Senften, M., Schwander, M., Kazmierczak, P., Lillo, C., Shin, J.B., Hasson, T., Geleoc, G.S., Gillespie, P.G., Williams, D., Holt, J.R., *et al.* (2006) Physical and functional interaction between protocadherin 15 and myosin VIIa in mechanosensory hair cells. *J. Neurosci.*, **26**, 2060–2071.
52. Selvakumar, D., Drescher, M.J. and Drescher, D.G. (2013) Cyclic nucleotide-gated channel alpha-3 (CNGA3) interacts with stereocilia tip-link cadherin 23 + exon 68 or alternatively with myosin VIIa, two proteins required for hair cell mechanotransduction. *J. Biol. Chem.*, **288**, 7215–7229.
53. Boeda, B., El-Amraoui, A., Bahloul, A., Goodyear, R., Daviet, L., Blanchard, S., Perfettini, I., Fath, K.R., Shorte, S., Reiners, J., *et al.* (2002) Myosin VIIa, harmonin and cadherin 23, three Usher I gene products that cooperate to shape the sensory hair cell bundle. *Embo J.*, **21**, 6689–6699.
54. Heissler, S.M. and Manstein, D.J. (2012) Functional characterization of the human myosin-7a motor domain. *Cell. Mol. Life Sci.*, **69**, 299–311.
55. Holme, R.H., Kiernan, B.W., Brown, S.D. and Steel, K.P. (2002) Elongation of hair cell stereocilia is defective in the mouse mutant whirler. *J. Comp. Neurol.*, **450**, 94–102.
56. Mathur, P.D., Vijayakumar, S., Vashist, D., Jones, S.M., Jones, T.A. and Yang, J. (2015) A study of whirlin isoforms in the mouse vestibular system suggests potential vestibular dysfunction in DFNB31-deficient patients. *Hum. Mol. Genet.*, **24**, 7017–7030.